Particles Versus Fibrillar Morphology in Polyolefin Ternary Blends

B. K. KIM* and I. H. DO

Department of Polymer Science and Engineering, Pusan National University, Pusan 609-735, South Korea

SYNOPSIS

PP/EPR binary and PP/(EPR/PE) ternary blends were prepared based on the viscosity ratio, using a corotating twin-screw extruder. Both fibrillar structures and particle-in-matrix morphologies were created depending on the viscosity ratio of rubber domain to the matrix PP(η_{EPR}/η_{PP}, or $\eta_{EPR\text{-}PE}/\eta_{PP}$). With fibril formation, mechanical properties of the blends, especially the flexural modulus and notched impact strength, were significantly increased and the increase was more pronounced with the ternary blends. The fractured surfaces obtained from the impact test showed compressed welded grains for fibrillar morphology and filled-out particles for particle-in-matrix morphology.

INTRODUCTION

Thermoplastic polyolefin (TPO) blends based on polypropylene (PP) are used extensively in a wide range of industrial end uses including automotive parts, wire, and cable coating.[1-3] Depending on the end use, rubber [typically the ethylene–propylene copolymer (EPM) and the ethylene–propylene–diene terpolymer (EPDM)] contents are varied 5–65%.[4-7] In one typical case, called thermoplastic vulcanizates (TPV), the rubber content is kept as high as possible (~ 65%) as long as PP forms a continuous phase.[8] In these blends, the rubber domains are partially or fully cured to ensure the basic rubberlike properties such as resilience and compression set. In TPV, high molecular weight rubber is employed to keep the rubber phase dispersed at high rubber loadings. Consequently, a high shear extruder is essential for blending.[8]

The other typical TPO which is considered in this article contains 20–30% rubber in PP. In this elastomer-modified thermoplastic, impact resistance is greatly enhanced and the coefficient of linear thermal expansion is retained at a low level. Regarding the morphology, rubber particles (~ 0.5 μm) are dispersed in the PP matrix and the matrix is toughened by a rubber-toughening mechanism.[9] Recently, a new concept was proposed based on the reversal of the current concept. Following Nomura et al.,[10,11] who used the PP copolymer [presumably carrying terminal ethylene–propylene blocks (EPM)], PP crystalline lamellas can be dispersed in a matrix consisting of networked amorphous PP and EPR.

In immiscible polymer blends, the properties greatly depend on the morphology, which, on the other hand, is governed by the chemical compositions and viscosity ratio of the base materials.[12-15] Therefore, we consider the morphology–property relationships of PP/EPR binary and PP/[EPR/polyethylene (PE)] ternary blends, based on the rheological properties of the base materials. Depending on the viscosity ratio of rubber domains to PP, both particle-in-matrix morphology and fibrillar structure were created. The rubber inclusion tensile modulus and the strength of PP are decreased. The magnitude of the tensile property decrease can be suppressed by adding PE into the rubber domains. In addition, PE can alter the viscosity ratio of the rubber domain to the PP phase, which could modify the rubber-phase morphology.

* To whom correspondence should be addressed.

Journal of Applied Polymer Science, Vol. 60, 2207–2218 (1996)
 CCC 0021-8995/96/122207-12

EXPERIMENTAL

The two types of isotactic PP, two types of high-density polyethylene (HDPE), three types of ultra-low-density polyethylene (ULDPE), and one type of EPR, listed in Table I, were used as received for blending. Blends were prepared by melt-mixing in a corotating twin-screw extruder (PEX-30, JSW) with $L/D = 30$, at 30 rpm using a temperature profile 210, 220, 230, and 220°C of first, second, third, and die zones, respectively. The rpm approximately corresponds to a shear rate of 200 s^{-1}. For PP/(EPR/PE) ternary blends, blending was done in two stages: The master pellet of PE(50)/EPR(50) (by weight) were first prepared to mix with PP in the second stage.

The morphology of the blends was observed using a scanning electron microscope (SEM, H-2700). Injection-molded tensile specimens were cryogenically (in liquid nitrogen) fractured, along the (L direction) and perpendicular (T direction) to the flow direction in the mold and etched with hexane. Fracture surfaces were sputtered with gold and examined under an SEM. The fractured surfaces of notched impact specimens were also examined under an SEM.

Rheological properties of the base resins and EPR were measured by a Rheometric dynamic spectrometer (RDS 7700) using a cone-and-plate fixture at 210°C, 15% strain level. RDS specimens were compression-molded. Figure 1 shows the melt viscosities of the base resins and EPR being used in the present experiment. Using these materials, two types of PP/EPR binary blends (runs a and A) and 10 types of PP/(EPR/PE) ternary blends (runs b–f and B–F) were prepared (Table II). In runs a–f, the viscosity of EPR is smaller than that of PP ($\eta_{EPR} > \eta_{PP}$), whereas $\eta_{PP} < \eta_{EPR}$ in runs A–F. The viscosity of PE is greater than that of EPR in b and c (also B and C) and is smaller in d–f (also D–F). Therefore, the viscosity of the rubbery domains can be increased and decreased depending on the type of PE added. The mechanical properties of the blends, hardness (Shore D), tensile and flexural properties, and Izod notched impact strength were determined using injection-molded specimens following the standard procedures described in ASTM. Injection was done under similar conditions with extrusion. The error ranges of the mechanical tests were 5–7% and the averages of at least three runs were taken.

RESULTS AND DISCUSSION

Morphology

Figure 2 shows the SEM morphologies of PP/EPR binary blends. The longitudinally fractured sample of run a shows highly elongated fibrills. On the other hand, run A shows simply deformed particles. With high elongation along the flow direction, the cross section of run a is much smaller than that of run A.

In steady shear flows, the deformation of a dispersed phase can be determined by two dimensionless parameters, viz., the viscosity ratio (λ) and the capillary number (κ) defined below[15,16]:

$$\lambda = \frac{\eta_d}{\eta_m} \tag{1}$$

$$\kappa = \frac{\eta_m \dot{\gamma}}{\nu/D} \tag{2}$$

where η_d and η_m are the viscosity of dispersed and continuous phases, respectively, and $\dot{\gamma}$, ν, and D are the shear rate, interfacial tension, and droplet

Table I Physicochemical Properties of Base Polymers

	Density (g/cm³)	T_m (°C)	MFI (g/10 min)	M_w (10^4 g/mol)	Comonomer	C_2 Unit	Producer
PP1	0.90	162	3.0	38	—	—	5014L, Korea Petrochemicals
PP2	0.90	163	7.5	25	—	—	4017, Korea Petrochemicals
EPR	0.867	—	—	—	—	76% wt	KEP020, Kumho
HDPE1	0.956	129	0.84	18.59	—	100% wt	E308, Korea Petrochemicals
HDPE2	0.96	136	4.8	9.66	—	100% wt	M850, Korea Petrochemicals
ULDPE1	0.893	82.0	3.9	6.99	1-Butene	86% mol	A4090, Mitsui Petrochemicals
ULDPE2	0.895	84.2	18.2	4.78	1-Butene	86% mol	A20090, Mitsui Petrochemicals
ULDPE3	0.865	40.8	0.4	14.20	4-Methyl 1-pentene	76% wt	P0480, Mitsui Petrochemicals

PP: MFI under 2.16 kg load at 230°C. HDPE and ULDPE: MFI under 2.16 kg load at 190°C.

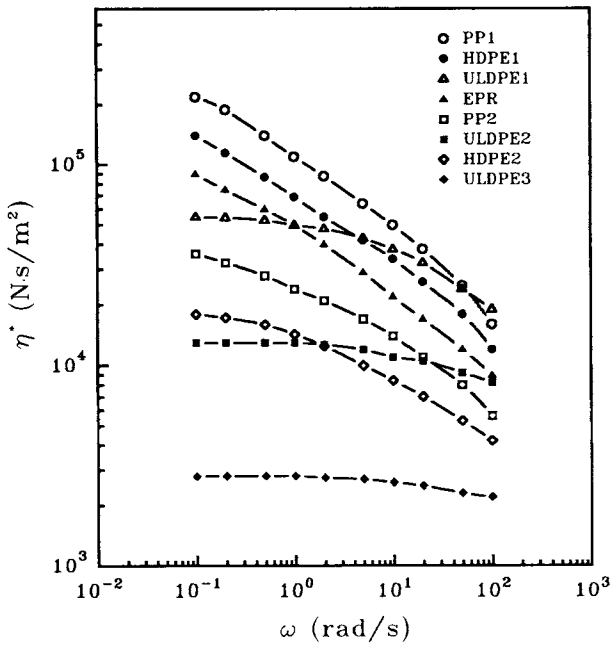

Figure 1 Melt viscosities of the base polymer.

diameter, respectively. The numerator of eq. (2) is the shear stress ($\sigma = \eta_m\dot{\gamma}$) imposed on the continuous phase by screw rotation, and this stress is transferred to the dispersed phase, with the magnitude determined by the interfacial conditions. Assuming shear stress continuity at the interfaces, the shear rate imposed on the dispersed phase is given by

$$\dot{\gamma}_d = \frac{\eta_m}{\eta_d}\dot{\gamma} \tag{3}$$

At a given screw rpm, the dispersed-phase deformability is inversely proportional to the viscosity ratio of dispersed phase to the continuous phase. Also, eq. (2) can be written as

$$\kappa = \frac{\eta_d\dot{\gamma}_d}{\nu/D} \tag{4}$$

Then, the numerator of eq. (4) is the driving force for the dispersed-phase deformation, the denominator is the interfacial stress which acts as the resistance against deformation, and deformation occurs only for κ greater than the critical value.

The fibrillation of dispersed domains occurs easily in the process of injection molding due to the high stress and rapid quenching. However, the conditions for fibril formation seem more complicated than for the droplet breakup. Fibrils were reported at $0.3 < \eta_d/\eta_m < 1.0$ for PE/polystyrene blends[17] and at $\eta_d/\eta_c > 3.7$ for poly(ethylene terephthalate)/polyamide blends.

In our experiments, run a corresponds to $\eta_d/\eta_m < 1$, and run A, to $\eta_d/\eta_c > 1$. It seems that the deformability is primary governed by the viscosity ratio [eq. (3)], and $\eta_d/\eta_c < 1$ seems necessary for fibril formation in PP/EPR blends.

Table II Basic Formulations of PP/EPR Binary Blends and PP/(EPR/HDPE) and PP/(EPR/ULDPE) Ternary Blends

Run	PP1	PP2	EPR	HDPE1	HDPE2	ULDPE1	ULDPE2	ULDPE3
a	70	—	30	—	—	—	—	—
b	70	—	15	15	—	—	—	—
c	70	—	15	—	—	15	—	—
d	70	—	15	—	15	—	—	—
e	70	—	15	—	—	—	15	—
f	70	—	15	—	—	—	—	15
A	—	70	30	—	—	—	—	—
B	—	70	15	15	—	—	—	—
C	—	70	15	—	—	15	—	—
D	—	70	15	—	15	—	—	—
E	—	70	15	—	—	—	15	—
F	—	70	15	—	—	—	—	15

Viscosity relation: No. 1 ⇒ EPR < PP. Nos. 2 and 3 ⇒ EPR < (HDPE or ULDPE) < PP. Nos. 4 and 5 ⇒ (HDPE or ULDPE) < EPR < PP. No. 7 ⇒ PP < EPR. Nos. 8 and 9 ⇒ PP < EPR < (HDPE or ULDPE). Nos. 10–12 ⇒ (HDPE or ULDPE) < PP < EPR.

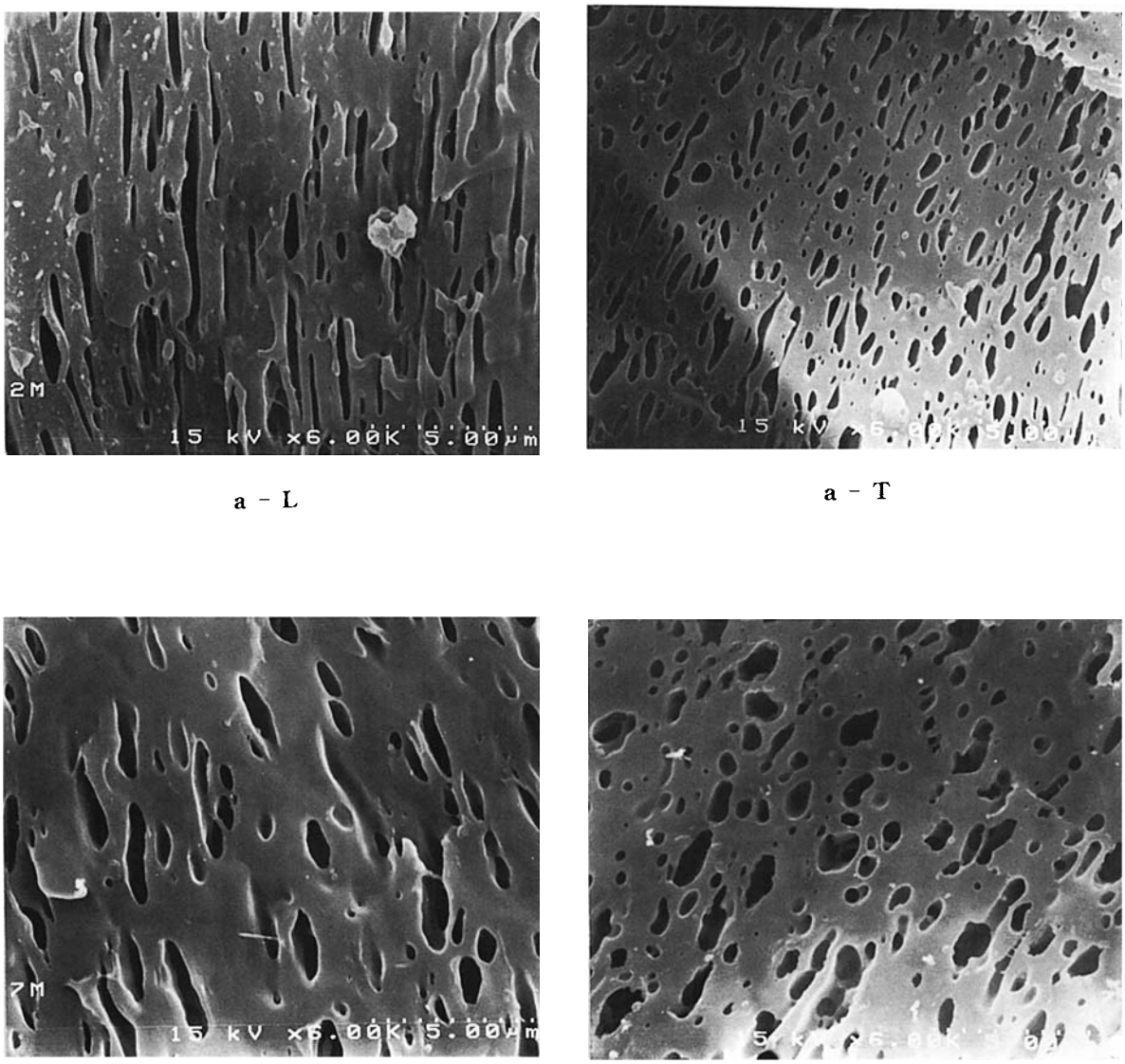

a - L a - T

A - L A - T

Figure 2 SEM micrographs of PP/EPR blends of runs a and A.

It seems that the effect of adding high viscosity PE ($\eta_{EPR} < \eta_{PE}$) to the PP/EPR binary blends largely depends on the viscosity ratio of EPR to PP. For $\eta_{EPR} < \eta_{PE}$, fibril formation becomes more feasible (Fig. 3, runs b and c), and for $\eta_{EPR} > \eta_{PE}$, the dispersed domains become rather larger (Fig. 4, runs B and C) with the addition of PE. This implies that PEs are preferentially dissolved in EPR domains and modify the rubber-phase viscosity. In Figure 3, the viscosity of the rubber domain is increased with PE addition, but it is still lower than that of PP ($\eta_{EPR-PE} < \eta_{PP}$). It is seen that ULDPEs have been etched out together with EPRs, and EPRs are interposed at the interfaces. On the contrary, in Figure 4, the viscosity of the EPR domain, satisfying $\eta_{EPR} > \eta_{PE}$, has been further increased with the addition of PE.

In Figures 5 and 6, PE with $\eta_{PE} < \eta_{EPR}$ was added to the binary blends (runs a and A). Regardless of the viscosity ratio of EPR to PP, fibrils are formed. This is primarily due to the lowered viscosity of the rubber domain. When the same type of PE was added, fibrillation seems more feasible for $\eta_{EPR} < \eta_{PP}$ (Fig. 5) than for $\eta_{EPR} > \eta_{PP}$ (Fig. 6). Among the three types of PE added, rubbery domains containing ULDPE 2, which has a sig-

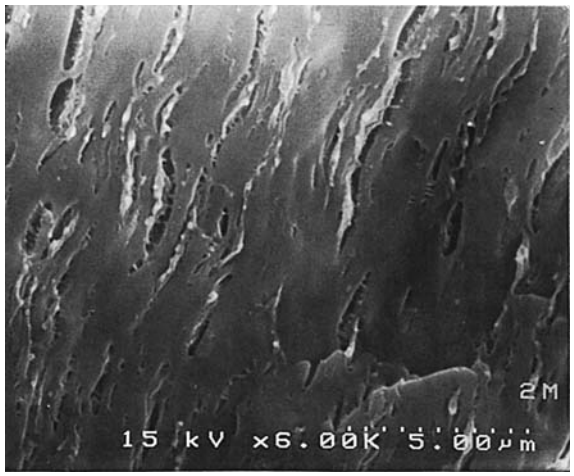

b - L

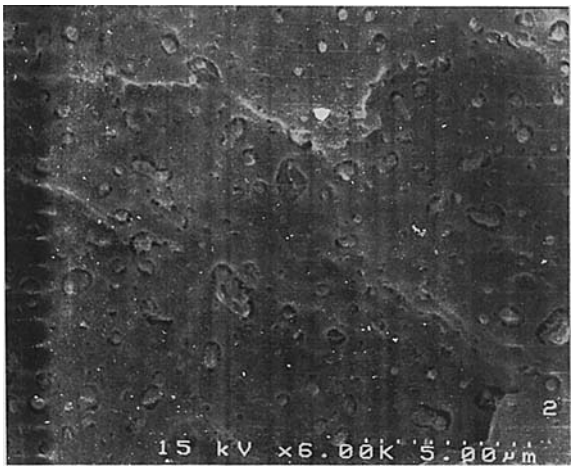

b - T

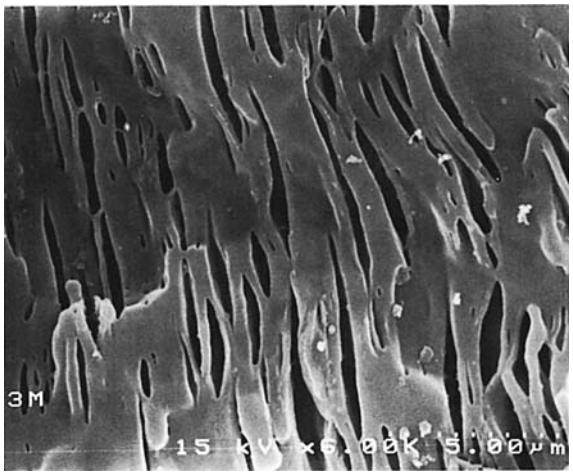

c - L

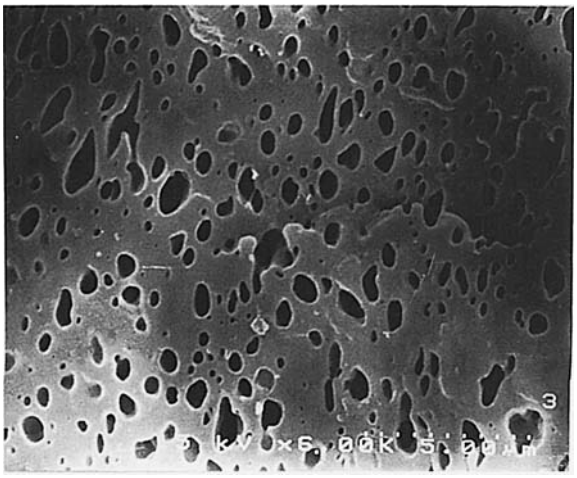

c - T

Figure 3 SEM micrographs of PP/(EPR/PE) ternary blends of runs b and c.

nificantly low viscosity, produced the most well-defined fibrils with a relatively large diameter. It seems that relatively large domains, allowing more shear stress transfer to the rubbery domains, are essential for complete stratification of the domains when the interfacial interactions are small, as in polyolefin blends.

Figures 7 and 8 show the typical fractured surfaces of the notched impact test. Depending on the domain morphology, significantly different fracture surfaces are obtained, especially near the unnotched surface, which is subject to compression during the test. The rubber domains are welded with the PP matrix when fibrils are formed; however, they are simply compressed particles with a particle-in-matrix morphology. The difference in fractured morphology should give a clue to the significantly different impact toughness to follow.

Mechanical Properties

In multiphase polymer blends, mechanical properties are often the response of morphology, which, on the other hand, is the response of rheology. Mechanical properties of these blends are tabulated

B - L

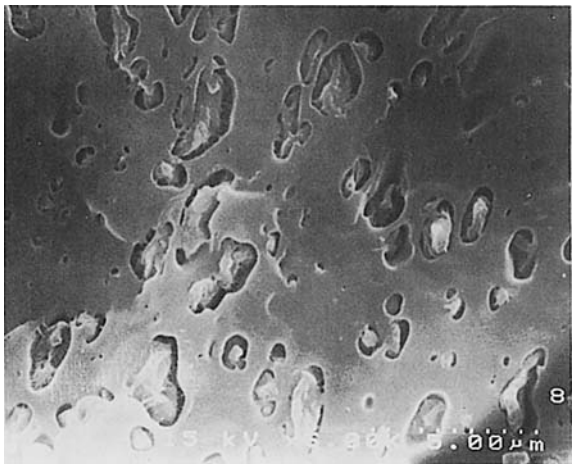

B - T

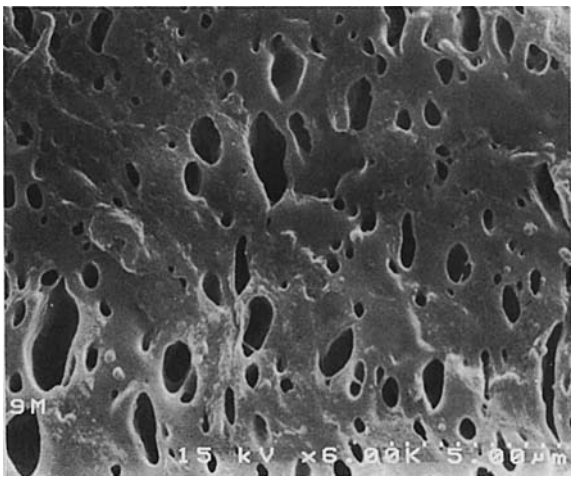

C - L

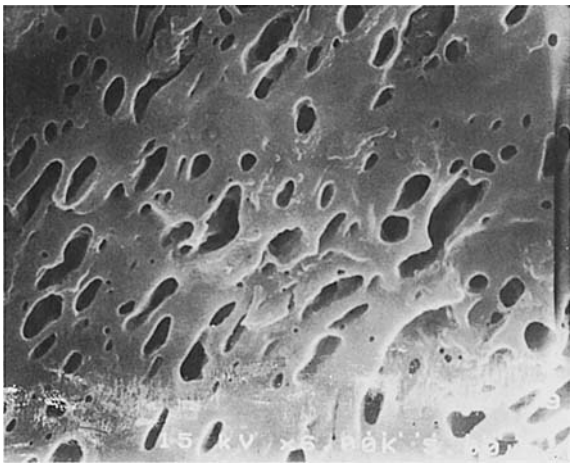

C - T

Figure 4 SEM micrographs of PP/(EPR/PE) ternary blends of runs B and C.

in Table III and Figures 9 and 10. The hardness, modulus, and strength of PP are decreased with the addition of rubber. However, the relative decrease of these properties greatly depends on morphology control. For example, the yield strength of PP is decreased from 33.7 to 19.7 MPa with fibril formation (run a) and from 37.6 to 17.3 MPa with particle formation (run A). However, the most pronounced morphology effects are obtained with a flexural modulus and impact strength (Fig. 9), which together are the key properties for automobile bumper applications. With fibril formation, over 70% of the flexural modulus of PP is retained with about a ninefold increase in impact strength. On the contrary, with particle formation, only 45% of the flexural modulus of PP is retained with about a fivefold increase in impact strength. Significantly, impact toughening of run a as compared to run A is in part due to the higher molecular weight of PP1 than that of PP2. However, the impact strengths of PP1 and PP2 are only 4.8 and 2.8 kg cm/cm, which makes little contribution to the impact strength of the PP/EPR blends (42.1 for run a and 14.7 kg cm/cm for run A). So, we can conclude that morphology mainly governs the impact strength of the blends.

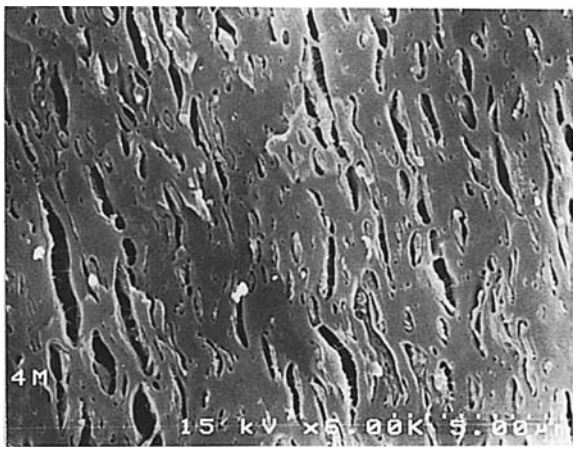

d - L

d - T

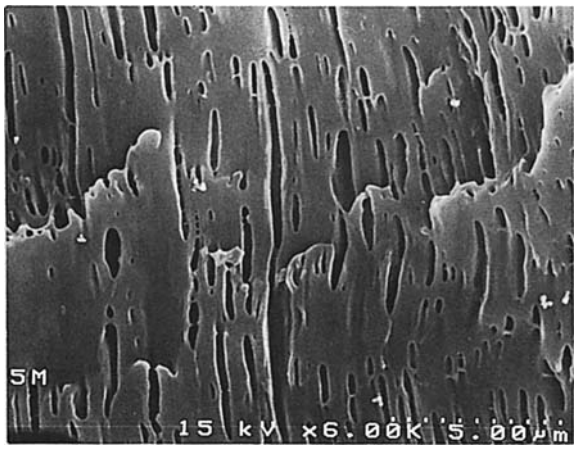

e - L

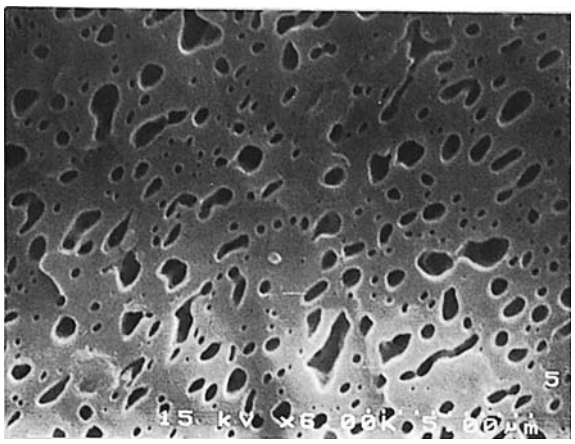

e - T

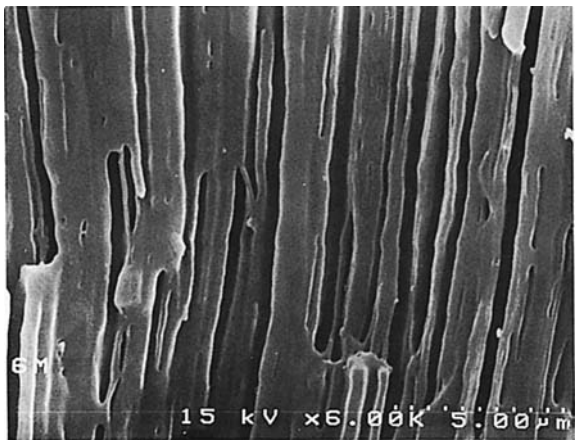

f - L

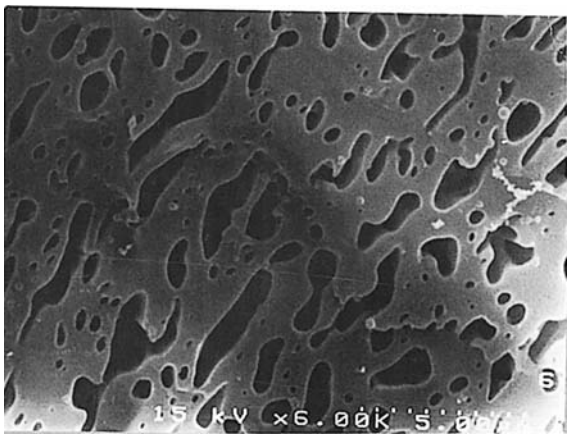

f - T

Figure 5 SEM micrographs of PP/(EPR/PE) ternary blends of runs d–f.

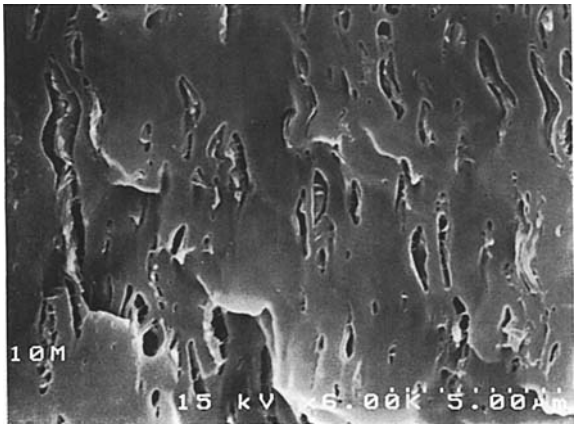

D - L

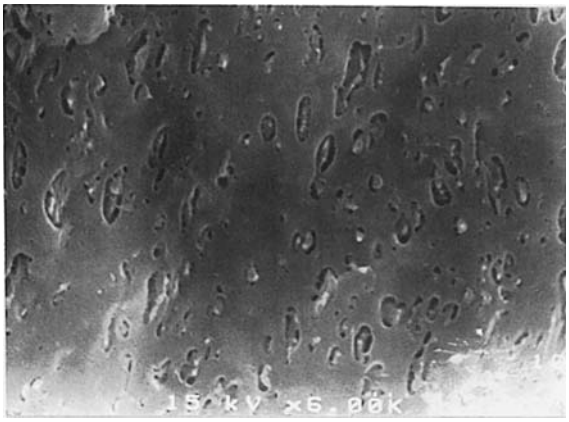

D - T

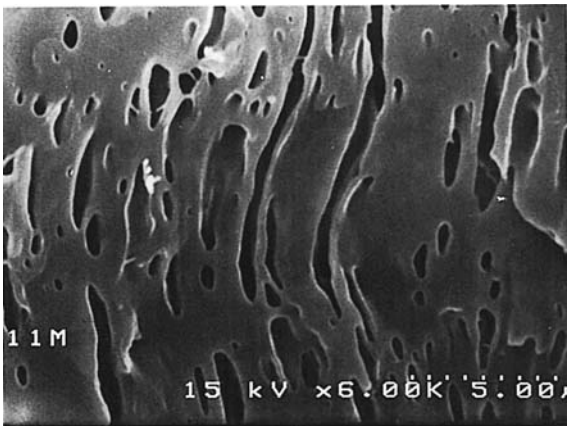

E - L

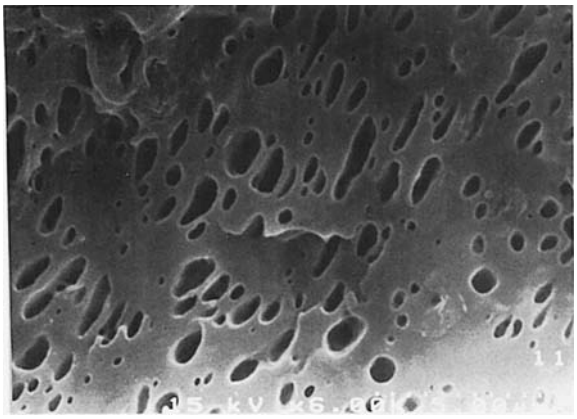

E - T

F - L

F - T

Figure 6 SEM micrographs of PP/(EPR/PE) ternary blends of runs D–F.

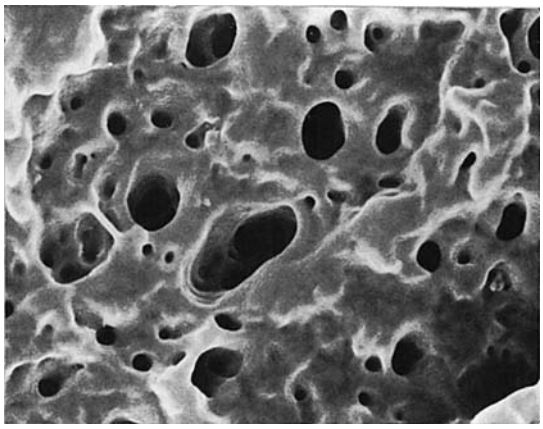

a - U

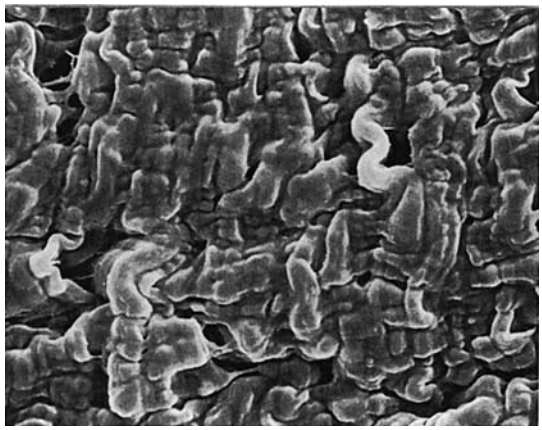

a - D

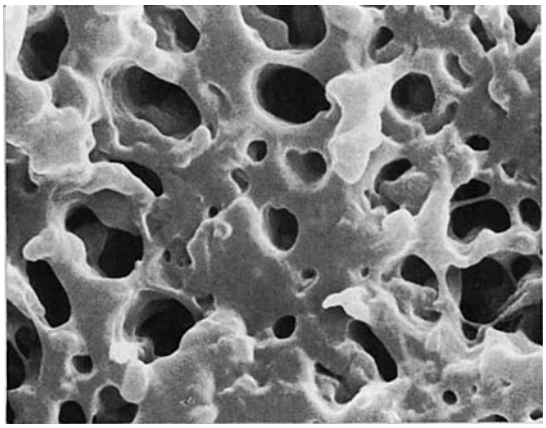

b - U

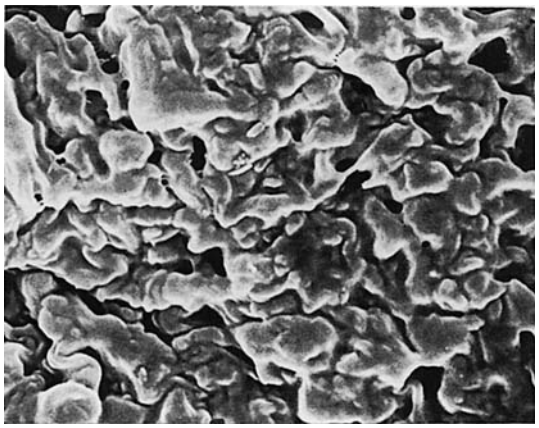

b - D

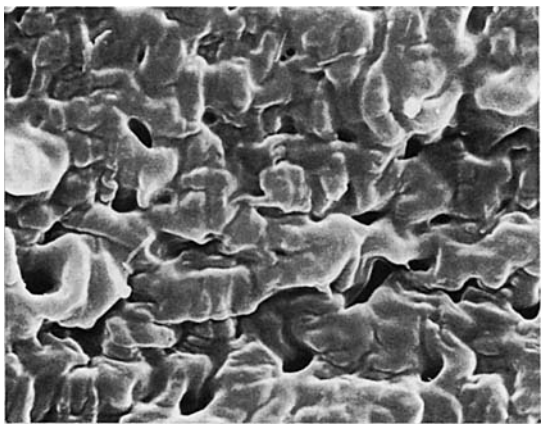

c - U

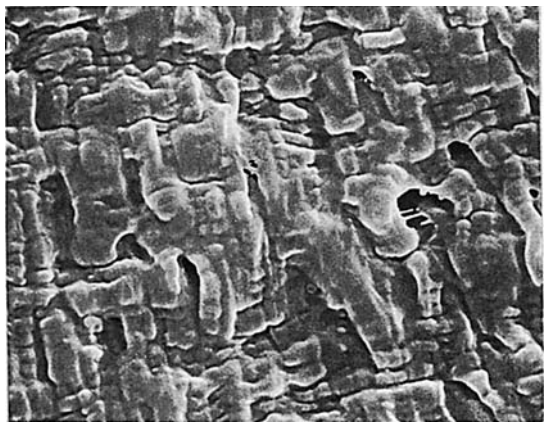

c - D

Figure 7 SEM micrographs of fractured surfaces of notched impact test of runs a–c.

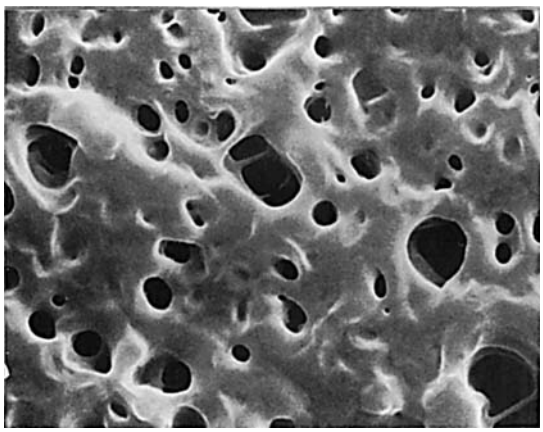

A - U

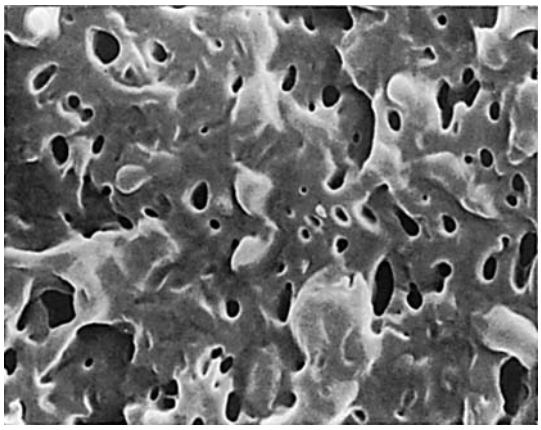

A - D

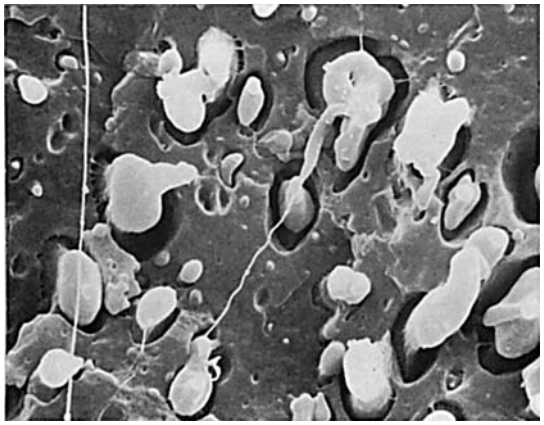

B - U

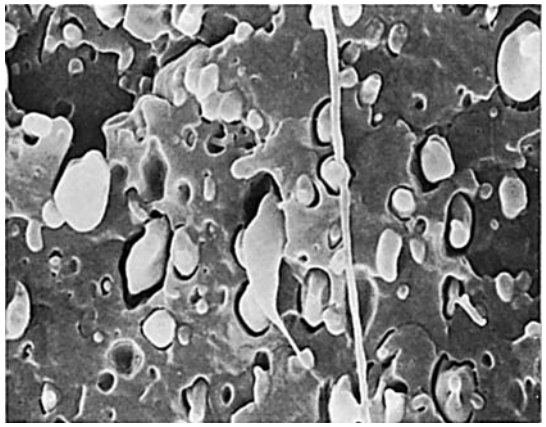

B - D

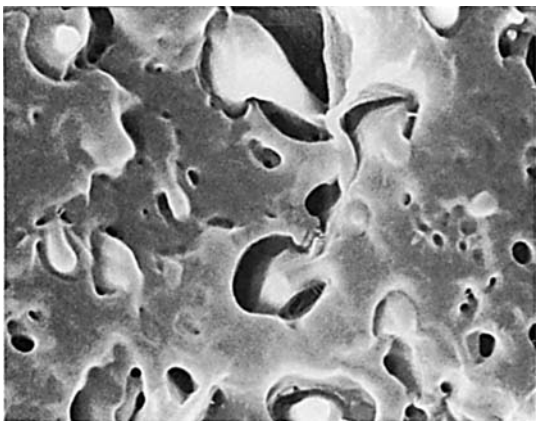

C - U

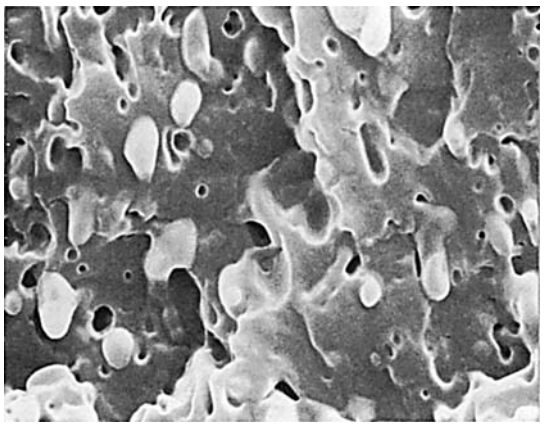

C - D

Figure 8 SEM micrographs of fractured surfaces of notched impact test of runs A–C.

Table III Mechanical Properties of PP/EPR Binary Blends and PP/(EPR/HDPE) and PP/(EPR/ULDPE) Ternary Blends

Run	I/S (kgf cm/cm)	F/M (MPa)	Y/S (MPa)	B/S (MPa)	ε_b (%)	Hardness (Shore D)
a	42.1	700.0	19.7	35.4	455	60.8
b	47.2	884.6	24.1	38.7	590	67.3
c	56.7	667.3	18.3	31.0	521	61.0
d	49.8	857.7	23.0	37.5	571	66.2
e	54.1	694.2	21.1	35.5	553	62.4
f	39.1	687.2	19.9	32.1	500	62.5
A	14.7	633.8	17.3	27.4	548	60.3
B	5.7	851.9	27.7	33.4	564	66.5
C	9.6	663.4	20.1	26.9	517	62.3
D	7.2	809.6	25.2	33.0	587	66.0
E	10.2	703.8	19.9	31.5	593	64.3
F	11.0	682.7	19.6	31.2	579	61.7
PP1	4.8	994.2	33.7	45.7	554	75.5
PP2	2.8	1390.3	37.6	45.4	585	76.2

I/S: notched impact strength. F/M: flexural modulus. Y/S: yield strength. B/S: break strength. ε_b: elongation at break.

It is seen that the impact strength of run C is greater than that of run B. This is due mainly to the relatively smaller particle size of C. Though an optimum particle size can exist, impact strength generally increases with the decrease of particle size.

The morphology effect is more pronounced in ternary blends. The impact strength of PP increased 8.1 (run f)–11.8 (run c) times with fibril formations, and it is 2.0 (run B)–3.9 (run F) times with particle formations (Fig. 10). The increase of flexural modulus is also significantly suppressed or even increased with fibril formation (Fig. 11). It is seen that ULDPE blends generally give better impact strength and poor modulus and strength as compared with HDPE blends. This is because ULDPE are copolymers with α-olefins and, consequently, they have low crystallinity and low molecular weight and contribute little in reinforcing the rubber domains.

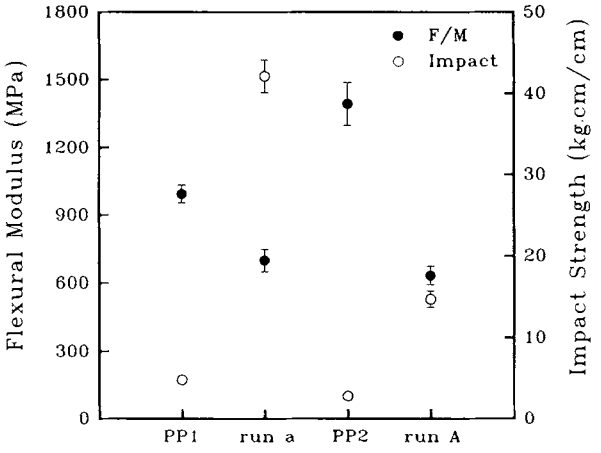

Figure 9 Flexural modulus and impact strength of PP/EPR binary blends (runs a and A).

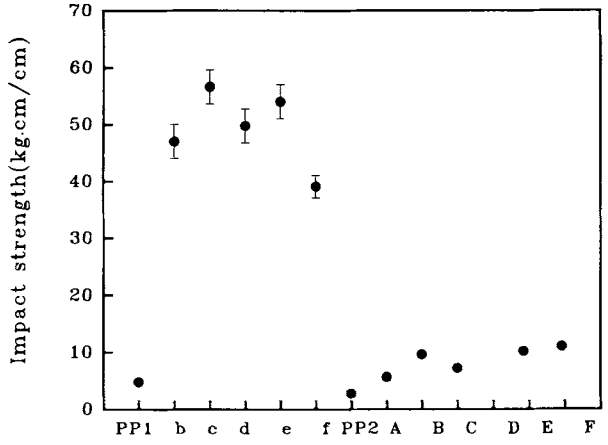

Figure 10 Impact strength of PP/(EPR/PE) ternary blends (runs b–f and B–F).

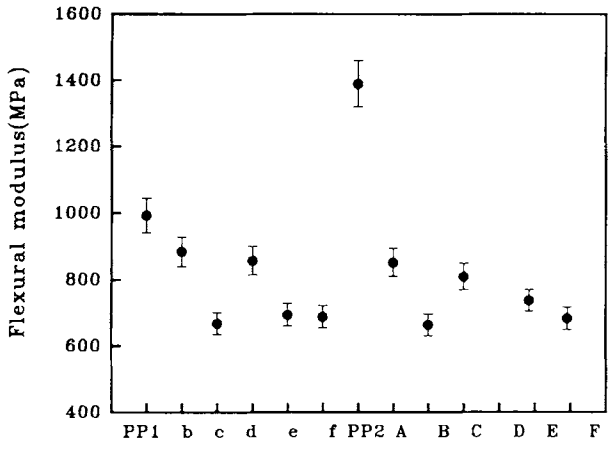

Figure 11 Flexural modulus of PP/(EPR/PE) ternary blends (runs b–f and B–F).

The financial support of the Korea Science and Engineering Foundation is gratefully acknowledged.

REFERENCES

1. J. Karger-Kocsis and I. Csikai, *Polym. Eng. Sci.*, **27,** 241 (1987).
2. A. P. Plochocki, in *Polymer Blends,* D. R. Paul and S. Newman, Eds., Academic Press, New York, 1987, Chap. 21.
3. E. N. Kresge, in *Polymer Blends,* D. R. Paul and S. Newman, Eds., Academic Press, New York, 1987, Chap. 20.
4. M. J. Flokes and P. S. Hope, Eds., *Polymer Blends and Alloys,* Blackie, London, 1993.
5. D. J. Synnott, D. F. Sheidan, and E. G. Kontos, in *Thermoplastic Elastomers from Rubber-Plastic Blends,* S. K. De and A. K. Bhowmick, Eds., Ellis Horwood, New York, 1990.
6. N. M. Mathew and A. J. Tinker, *J. Nat. Rubb. Res.,* **1,** 240 (1986).
7. D. Hoppner and J. H. Wendorff, *Colloid Polym. Sci.,* **268,** 500 (1990).
8. Monsanto, U.S. Pat. 4,311,628 (1982).
9. C. B. Bucknall, *Toughened Plastics,* Applied Science, London, 1982.
10. T. Nomura, T. Nishio, H. Sato, and H. Sano, *Kobunshi Ronbunshu,* **50**(1), 19 (1993); **50**(1), 27 (1993); **50**(2), 81 (1993); **50**(2), 87 (1993); **51**(9), 569 (1994); **51**(9), 577 (1994).
11. T. Nomura, T. Nishio, T. Yokoi, and H. Iwai, Society of Automotive Engineers International, Global Mobility Database SP-902, 1992.
12. C. D. Han, *Multiphase Flow in Polymer Processing,* Academic Press, New York, 1989.
13. L. A. Utracki, *Polymer Alloys and Blends,* Hanser, New York, 1989.
14. B. K. Kim, M. S. Kim, and K. J. Kim, *J. Appl. Polym. Sci.,* **48,** 1271 (1993).
15. L. A. Utracki, M. M. Dumoulin, and P. Toma, *Polym. Eng. Sci.,* **26,** 34 (1986).
16. L. A. Utracki and Z. H. Shi, *Polym. Eng. Sci.,* **32,** 1824 (1992).
17. M. Kim and J. L. White, *Polym. Eng. Sci.,* **23,** 1327 (1984).
18. W. Beger, H. W. Kammer, and C. Kummerlowe, *Macromol. Chem.,* **8,** 102 (1984).

Received August 22, 1995
Accepted December 16, 1995